

Three-Dimensional Reconstruction of Lymphatics Using a Crown-Rump Length 30 mm Human Fetus

Shu Huang^{1#}, Hechen Zhang^{1#}, Peng Zhao¹, Xinlin Chen², Gen Yan^{3}, Zhe-Wu Jin^{1*}*

ABSTRACT

Few lymphatic morphological studies have been conducted to describe human development compared to the number of vascular studies. In this study, serial sections from a 30-mm human fetus were used to observe the differentiation of the lymphatics and blood vessels through D2-40 immunohistochemical staining and three-dimensional reconstruction to reflect the morphological characteristics. We found a connection between the lymphatics of the left jugular lymph sac flowing into the left brachiocephalic vein but not between the thoracic duct (TD) and left venous angle. We found a lymphatic plexus in the sacral region, which was located between L4 and S1. Moreover, a pair of paravertebral longitudinal lymphatics originated near the cisterna chyli and collected lymphatics that accompanied the posterior intercostal blood vessels and finally flowed into the TD. The volume of jugular lymph sac, the left side had a slightly greater than that of the right side. In contrast, the venous system on the right side had a greater advantage than that on the left. In addition, a pair of paravertebral longitudinal lymphatics may have been described as the thoracic duct.

INTRODUCTION

The lymphatic system is an essential secondary vascular system that is responsible for key functions such as interstitial pressure regulation, immune cell trafficking, and dietary fat absorption Cueni et al. (2008). In contrast to blood vessels, few studies have investigated the morphological development of the lymphatics in human embryos and fetuses. Currently, the classic depiction of human fetal lymphatic vessels was drawn by Sabin et al. (1909). Also, Sabin's proposing of lymphatic vasculature has a venous origin and is derived from primitive lymph sacs scattered along the embryonic body axis was recently validated using a genetic lineage-tracing approach after more than a century. Usually, the lymphatics form after the development of blood vessels at a gestational age (GA) of six weeks, and six primary lymph sacs continue to develop and are connected by self-proliferation and polarized sprouting. Although Kampmeier et al. (1912) and van der Putte et al. (1975) described and drew detailed descriptions of the developmental morphology of the lymphatics in embryos, a more visual image description is needed.

At present, a three-dimensional (3D) digital atlas and database of human embryos has been established by de Bakker et al. (2016),

but it does not include the lymphatics. Immunohistochemical (IHC) staining could distinguish between lymphatic vessels and blood vessels. Podoplanin (D2-40) is a highly effective expressed in lymphatic endothelial cells but not in vascular endothelial cells, and D2-40 considered as a specific marker of capillary lymphatic vessels used for pathological diagnosis (Yokomori et al. (2010); Xie et al. (2018); Jeong et al. (2022)). Due to the limited morphological data of lymphatic development, it is necessary to combine the IHC technique with 3D reconstruction to study lymphatic connections, which is essential to understand organogenesis. Consequently, the aim of the present study was to use immunohistochemistry to confirm the relationship between the lymphatic connections and blood vessels and to reconstruct these structures to clarify the morphological characteristics of the lymphatics during development.

MATERIALS AND METHODS

This study was performed in accordance with the provisions of the Declaration of Helsinki 1995 (as revised in 2013). In this study, we used a human fetus with a crown-rump length (CRL) of 30 mm,

¹Department of Anatomy, Wuxi School of Medicine, Jiangnan University, Wuxi, China

²Department of Ultrasonography, Maternal and Child Health Hospital of Hubei Province, Tongji Medical College, Huazhong University of Science and Technology, Wuhan, China

³Department of Radiology, The Second Affiliated Hospital of Xiamen Medical College, Xiamen, China

Correspondence to: Zhe-Wu Jin, Department of Anatomy, Wuxi School of Medicine, Jiangnan University 1800 Lihu Avenue, Wuxi, Jiangsu, 214122, China.

E-mail: zwjin@jiangnan.edu.cn, Tel: +86) 510-8519-7079; Fax: +86) 510-8519-3570.

Keywords: lymphatic vessel; D2-40; human fetus; 3D reconstruction

obtained by induced abortion, after which the mother was orally informed (no paper signature) by an obstetrician at the college teaching hospital of the possibility of donating the fetus for medical research. The specimen was donated to Department of Anatomy, Yanbian University School of Medicine, and the use of research was approved by the university ethics committee (BS-13-35). Ethics approval for the use of fetuses has been published previously (Rodríguez-Vázquez et al. 2018). The Medical Ethics Committee of Jiangnan University also approved the use of serial sections for this study (JNU20190318IRB62).

Routine histology

The specimen was stored in 10% w/w neutral formalin solution for more than 1 month, decalcified by incubating at 4 °C in 0.5 mol/L ethylenediaminetetraacetic acid (pH 7.5) solution for three days, dehydrated with a graded series of ethanol, and routinely imbedded in paraffin. A total of 1018 sagittal serial section slides (5 µm in thickness) were obtained with an interval of 10 µm. We selected 505 slides for hematoxylin-eosin (HE) staining (the No. 2, 4, 8, and 10 out of every ten) and anti-podoplanin (D2-40) staining (the No. 6 out of every ten) to observe the lymphatic vessels more accurately. D2-40 IHC analyses were performed by incubating with the primary antibody (anti-podoplanin, 1:1000 dilution, Abcam, Cambridge, UK) overnight at 4 °C. The next day, sections were incubated with the secondary antibody (goat anti-rabbit polyclonal antibody; 1:100 dilution, Abcam, Cambridge, UK) labeled with horseradish peroxidase at 37 °C for 30 min. Sections were then stained with 3,3'-diaminobenzidine (DAB kit, ZLI-9022, ZSGB-BIO, China) to reveal the antigen-antibody complexes.

Three-dimensional reconstruction

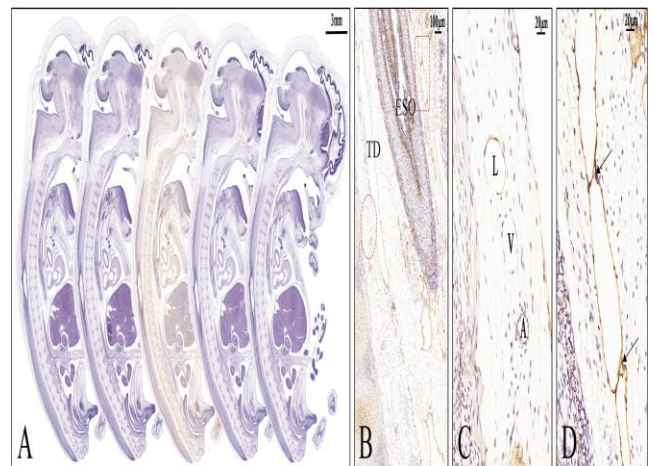
The stained slides were scanned using a Panoramic MIDI (3D Histech, Hungary) scanner to observe the high-quality full-width seamless connection microscope structure of the lymphatics and the vasculature through software (Case Viewer 2.4.0, 3D Histech, Hungary), with a total of 657 gigabytes of data. The images were exported in TIF format at a ratio of 1:8 for reconstruction, and the Pathon code in Pycharm was run to unify the pixel size of the picture and convert it into grayscale images. Grayscale images are automatically registered with adjacent images (X, Y, and Z axes) through Align Slices-Edit-Align. All slices were processed with the Amira 6.2 program (Thermo Fischer Scientific Inc., U.S.A.), and adjacent layers with large deviation were registered by manual rotation. After completing the image registration, the two-dimensional images were imported into the 3D reconstruction software of Mimics 21.0 (Materialise, Belgium). After manually drawing (Edit mask), the structural contours of the lymphatic vessels, veins, and arteries are depicted layer by layer to ensure that the edges of the mask are consistent with the edges of the structure and to ensure the accuracy

of the drawing. After drawing, the 3D model was generated by the Calculate part command, and the model quality was selected as optimal. The data were exported in STL format. The 3D model was imported into GeomagicStudio12 for model smoothing and noise reduction.

RESULTS

Distribution of lymphatics can be clearly distinguished by D2-40 IHC staining. The HE and D2-40 IHC staining ratio was 4:1, with each D2-40 IHC result as the center, and lymphatic vessel connections were carefully observed on both sides of the HE-stained slides (Fig. 1A). D2-40 positive was good at distinguishing lymphatic vessels with blood vessels (Fig. 1B-D).

Figure 1: Distinguish lymphatic vessels with blood vessels.



Sagittal sections. (A) Select four Hematoxylin-Eosin staining and one D2-40 immunohistochemical staining from every 10 serial sections for scanning. (B) Low magnification observation of near esophagus (Eso) and thoracic duct (TD). (C) High magnification observation of the red oval line in B. L, lymphatic vessel; V, vein; A, artery. (D) High magnification observation of the red rectangular line in B. Arrows indicate lymphatic connections. The magnification of each panel refers to the scale bar in upper right corner.

In addition, D2-40 IHC staining also easy to found lymphatic connections and valves. We observed a typical connection between lymphatic vessels and valves flowing into the left brachiocephalic vein (Fig. 2).

Based on the 3D reconstruction of blood vessels and lymphatic vessels, in this period, most positive lymphatics were clearly observed near blood vessels. In the cervical and lumbar regions, we found dense lymphatics fused with blood vessels in this area, and lymphatics filled in the space between veins and arteries (Fig. 3). In our study,

Figure 2: Connection between lymphatics and veins.

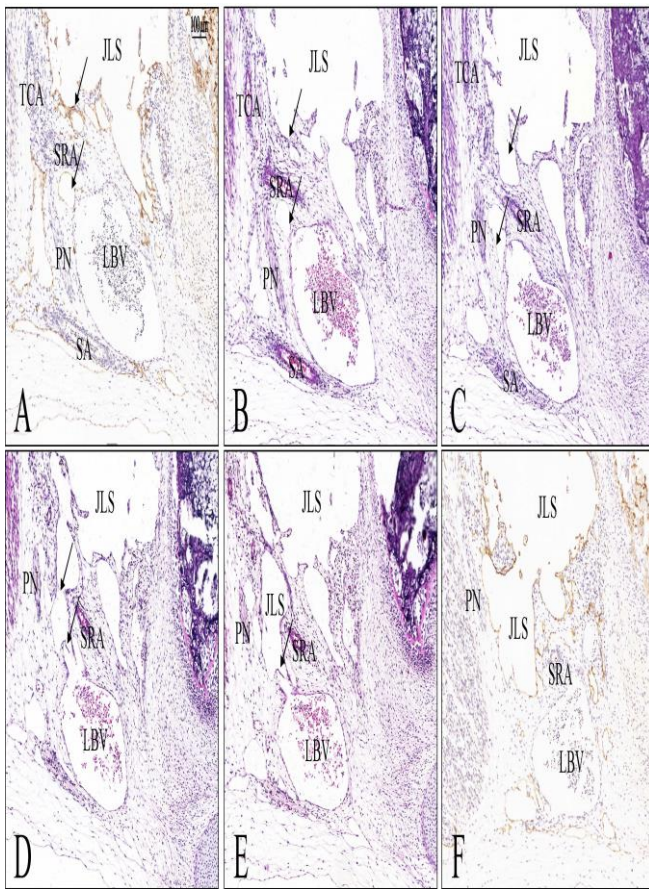
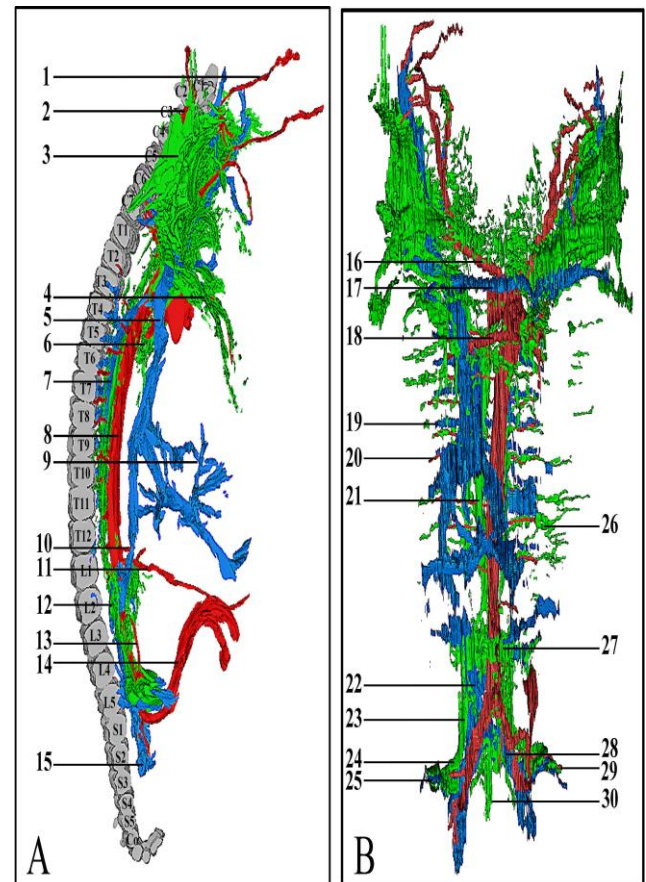


Figure A-E showed the morphological characteristics of some lymphatics and valves of jugular lymph sac (JLS) flowing into the left brachiocephalic vein (LBV). The arrows indicated lymphatics and valves. TCA, transverse cervical artery; SRA, suprascapular artery; PN, phrenic nerve; SA, subclavian artery. All panels are prepared at the same magnification (scale bar in A).

the left and right side of jugular lymph sac (JLS) were located above the lateral side of the left brachiocephalic vein. Each JLS occupied the majority of the lateral side of the first cervical vertebra (C1) to the C6 area. The volume of left JLS was 2.53 mm³, the right JLS volume was 1.930 mm³, and the L/R ratio was 1.311. The azygos vein flowed into the superior vena cava (SVC) on the right side of the aorta at the third thoracic vertebra (T3) level. The TD connected with the cisterna chyli (CC) and ran along the azygos vein from the right and posterior sides of the aorta. It turned slightly from the right to the left side at the T8-9 level and connected with the left JLS at the C6 level. According to our results, we did not find a clear point of connection between the TD and near the left venous angle, although they were mixed together in this area. The superior mesenteric artery (SMA) extended straight forward to the abdomen at the first lumbar vertebra (L1) level (Fig. 3A). We found that the intrathoracic lymphatic plexus and paratracheal lymphatic plexus were located in the anterior and posterior

mediastinum, respectively, and connected with the left and right JLS. In the lumbar region, the CC lies on the anterior side of L2, and the inflow to both sides of the lumbar lymphatic plexus (LLP) and iliac lymphatic plexus (ILP), retroperitoneal lymphatic plexus (RLP) or mesenteric lymphatic plexus also flowed into the CC. The CC was located between L1 and L3. We found a lymphatic plexus in the sacral region, the so-called sacral lymphatic plexus (SLP), which was located between L4 and S1. Both sides of the ILP were located at the level of L5.

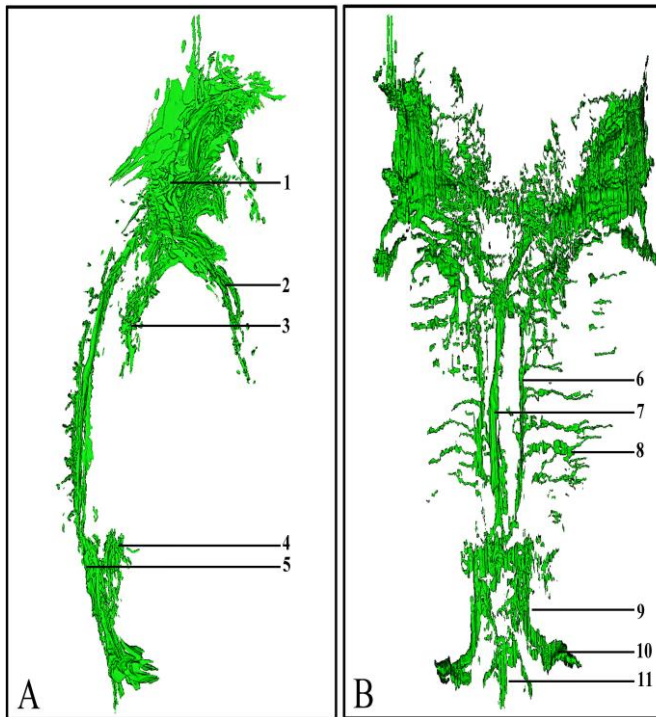
Figure 3: Reconstructed lymphatics and blood vessels.



1. Carotid artery; 2. Vertebral artery; 3. Jugular lymph sac;
4. Intrathoracic lymph plexus; 5. Superior vena cava; 6. Paratracheal lymph plexus; 7. Azygos vein; 8. Aorta; 9. Intrahepatic vessels; 10. Coeliac trunk; 11. Superior mesenteric artery; 12. Cisterna chyli; 13. Inferior mesenteric artery; 14. Umbilical arteries; 15. Iliac veins;
16. Brachiocephalic trunk; 17. Left brachiocephalic vein; 18. Pulmonary trunk and arteries; 19. Posterior intercostal veins; 20. Posterior intercostal arteries; 21. Thoracic duct; 22. Inferior vena cava; 23. Lumbar lymph plexus; 24. Iliac lymph plexus; 25. External iliac vein; 26. Posterior intercostal lymphatic vessels; 27. Retroperitoneal lymph plexus; 28. Common iliac vein; 29. External iliac artery; 30. Sacral lymphatic plexus.

In addition, except for the TD, a pair of longitudinal lymphatics on both sides of the spine, which originated near the CC, collected lymphatics that accompanied the posterior intercostal blood vessels during the ascending process and flowed into the TD (Fig. 4).

Figure 4: Reconstructed lymphatic vessels.



The black arrows indicate longitudinal lymphatics and the white arrow indicate posterior intercostal lymphatic vessels. 1. Jugular lymph sac; 2. Intrathoracic lymph plexus; 3. Paratracheal lymph plexus; 4. Retroperitoneal lymph plexus; 5. Cisterna chyli; 6. Paravertebral lymphatic trunks; 7. Thoracic duct; 8. Posterior intercostal lymphatic vessels; 9. Lumbar lymph plexus; 10. Iliac lymph plexus; 11. Sacral lymphatic plexus.

DISCUSSIONS

The lymphatic system is crucial for the immune response, and understanding its development might allow us to gain some insights into some human diseases, but little is known about human lymphangiogenesis during the embryonic and fetal periods. In humans, fatal embryonic edema was reported in nonimmune fetal edema, which was caused by congenital lymphatic dysplasia Wagner et al. (2022). Therefore, it is important to understand the development and morphological evolution of the lymphatics.

Although only a single fetal specimen was examined in this study, we selected a 30-mm CRL human fetus for serial sectioning for IHC and mainly compared it with Sabin's results [2] to further understand the morphological structure of the lymphatics at this stage. D2-40 is a mucin-type transmembrane glycoprotein that is effectively expressed in lymphatic endothelial cells

Adamczyk et al. (2016), and according to our previous results, it was also effectively expressed in human fetal specimens (Jin et al. 2010). Compared with previous research, D2-40 IHC staining could more specifically identify endothelial cells between lymphatics and the vasculature.

Through 3D reconstruction, the developing structures are easy to depict, allowing the reader to form an independent assessment de Bakker et al. (2016) compared to hand drawings. Regarding lymphatic development, textbooks usually describe early lymphatic capillaries as forming a network and becoming six primary lymph sacs at the end of the embryonic period. Next, mesenchymal cells invade each lymph sac and form a lymphatic channel of the primordia of the lymph sinuses, and other mesenchymal cells are transformed into lymph nodes in the early fetal period Moore et al. (2016). Except for JLS, we used the term lymphatic plexus instead of lymphatic sac or lymphatic channel in this study.

We found that the left brachiocephalic vein runs transversely and flows into the SVC from the left side. Both the left and right JLS were located above the left brachiocephalic vein. The lymphatics in both axillary regions were located at the lower edge of the left brachiocephalic vein, each ascending and flowing into the left or right JLS. According to previous results, when the embryos have reached a length of 30 mm, new and definitive lymphatico-venous communications are established at the jugulo-subclavian confluence van der Putte et al. (1975). In our results, we clearly found that the lymphatics from the JLS flowed into the left brachiocephalic vein. The JLS was located bilaterally at the levels between C1 and C6, and the volume was larger than that of the other lymphatic plexuses. According to 3D reconstruction results, the volume of left JLS was larger than the right JLS. These results indicated that our results were slightly different results of Carnegie stages 20 and 21 Ohga et al. (2020). As our reconstructed results, the venous were right side looks thicker and more branches than left side.

Both sides of the JLS extended into the thorax during this period and formed a connection with the anterior intercostal lymphatics through the parasternal lymphatics. The side of the paratracheal lymphatic plexus was located at the level of the ductus arteriosus to the tracheal bifurcation, and the lymphatics were connected to each other. It was not difficult to observe from the 3D results that the growth of the lymphatics followed that of blood vessels. According to the reconstruction, each side of the ILP flowed into the same side of the LLP, the SLPs were connected with both sides of the LLP, and these plexuses with the RLP flowed into the CC at the L2 level.

There was a renal vein passing through between the ILP and RLP. Regarding the SLP, van der Putte (1975) described that the RLP extends to the bifurcation of the aorta or, as observed more often, farther caudally as far as the area ventral to the caudal (sacral) veins. The TD originated from the CC and flowed into the left JLS. All of these results were consistent with those of previous studies. In this study, we found a pair of longitudinal paravertebral lymphatics on both sides of the spine. The left longitudinal lymphatics originated from the CC and received the left side of the posterior intercostal lymphatics and flowed into the thoracic duct at the T3-T4 level. The right longitudinal lymphatics originated from the TD at T11 and received the right side of the posterior intercostal lymphatics and flowed into the thoracic duct at the T4-T5 level. Longitudinal lymphatics were found accompanying the sympathetic trunk in mice (Wilting et al. 2022), and such paravertebral lymphatics may explain why the blockage/ligation of the thoracic duct in humans is well tolerated and does not necessarily produce lymphedema (Takhellambam et al. 2021). The paravertebral longitudinal lymphatics were concluded in other results (van der Putte 1975), but these were identified as the TD.

In this study, we used 3D reconstruction to fully demonstrate the morphological structure of the 30-mm human fetal lymphatics and conducted a more appropriate analysis compared to previous results. This information helps researchers and clinicians engaged in lymphatic development to provide basic morphological data.

CONCLUSIONS

We consider that the left lymphatics had a slightly greater advantage than the right lymphatics, similar to the left JLS volume being larger than the right. In contrast, the venous system on the left had a greater advantage than that on the right. In addition, we found a pair of paravertebral longitudinal lymphatics on both sides of the spine, similar to mice, but previously described as the TD.

DECLARATIONS

Acknowledgements

This work was supported by Wuxi Municipal Bureau on Science and Technology (Grant No. N20202008) and Zhangjiagang Science and Technology Innovation Project (Grant No. ZKCXY2123) in China.

REFERENCES

1. Cueni L N, Detmar M. 2008. The lymphatic system in health and disease. *Lymphat Res Biol.* 6(3-4):109-22.
2. Sabin F R. 1909. The lymphatic system in human embryos, with a consideration of the morphology of the system as a whole. *Am J Anat.* 9:43-91.

3. Srinivasan R S, Dillard M E, Lagutin O V, et al. 2007 Oct 1. Lineage tracing demonstrates the venous origin of the mammalian lymphatic vasculature. *Genes Dev.* 21:2422-2432.
4. Kampmeier O F. 1912. The value of the injection method in the study of lymphatic development. *Anat Record.* 6:223-232.
5. van der Putte S C. 1975. The development of the lymphatic system in man. *Adv Anat Embryol Cell Biol.* 51(1):3-60.
6. de Bakker BS, de Jong KH, Hagoort J, et al. 2016 Nov 25. An interactive three-dimensional digital atlas and quantitative database of human development. *Science.* 354(6315): aag0053.
7. Yokomori H, Oda M, Kaneko F, et al. 2010 Nov 8. Lymphatic marker podoplanin/D2-40 in human advanced cirrhotic liver- Re-evaluations of microlymphatic abnormalities. *BMC Gastroenterol.* 10:131.
8. Xie C, Wang R, Saeed A F U H, et al. 2018 Jul 5. Preparation of anti-human podoplanin monoclonal antibody and its application in immunohistochemical diagnosis. *Sci Rep.* 8(1):10162.
9. Jeong D P, Hall E, Neu E, et al. 2022 Aug 6. Podoplanin is responsible for the distinct blood and lymphatic capillaries. *Cell Mol Bioeng.* 15(5):467-478.
10. Rodríguez-Vázquez J F, Jin ZW, Zhao P, et al. 2018. Development of digastric muscles in human fetuses: a review and findings in the flexor digitorum superficialis muscle. *Folia Morphol (Warsz).* 77(2):362-370.
11. Wagner T, Fahham D, Frumkin A, et al. 2022 Jun. The many etiologies of nonimmune hydrops fetalis diagnosed by exome sequencing. *Prenat Diagn.* 42(7):881-889.
12. Adamczyk L.A, Gordon K, Kholová I, et al. 2016 Jul. Lymph vessels: the forgotten second circulation in health and disease. *Virchows Arch.* 469(1):3-17.
13. Jin ZW, Nakamura T, Yu HC, et al. 2010 Jun. Fetal anatomy of peripheral lymphatic vessels: a D2-40 immunohistochemical study using an 18-week human fetus (CRL 155 mm). *J Anat.* 216(6):671-82.
14. Moore K L, Persaud TV N, Torchia M G. 2016. Before we are born: essentials of embryology and birth defects. 9th Ed. Philadelphia Saunders.
15. Ohga A, Sakamoto R, Yamada S, et al. 2020 Mar. Vesicular swelling in the cervical region with lymph sac formation in human embryos. *Congenit Anom (Kyoto).* 60(2):62-67.

16. Wilting J, Becker J. 2022 Sep 15. The lymphatic vascular system: much more than just a sewer. *Cell Biosci.* 12(1):157.

17. Takhellambam L, Yadav T D, Kumar H, et al. 2021 Nov. Prophylactic ligation of the opacified thoracic duct in minimally invasive esophagectomy—feasibility and safety. *Langenbecks Arch Surg.* 406(7):2515-2520.